Thermal Expansion & Helical Buckling of Pipe-in-Pipe Flowline Systems

Brian W. Duffy, Liang-Hai Lee, and Mark Brunner

Genesis

Abstract:

Helical buckling analyses are performed primarily to determine the critical effective axial load at which the inner pipe of a pipe-in-pipe (PiP) system snaps into a sinusoidal or helical buckling deformation mode. The expected behavior, when a flowline is compressed within a larger diameter tubular, is that it will first develop a sinusoidal buckle pattern as it lies along the bottom of the larger diameter pipe. Further compression of the inner pipeline will ultimately cause it to snap into a helical deformation pattern, which will lift the inner flowline off of the bottom of the outer pipe. The axial force that triggers the sinusoidal buckling is denoted as F_{cs} and the larger force needed for helical buckling is denoted as F_c. However the majority of PiP systems use centralizers to hold the inner pipe in a, more or less, coaxial alignment with the outer pipe. The presence of such centralizers eliminates the possibility of the inner pipe to buckling in either mode.

The impact of one of the potential sources of geometric perturbation of the inner flowline, namely sleeper pipe upsets, was studied in this helical buckling analysis. The disturbance caused by the presence of a 0.75m high sleeper reduces the value of F_{cs} (as compared to a flat, perfect geometry) by approximately 33%. The sinusoidal buckling deflections of the inner pipe of the PiP system are severe enough to cause global lateral buckling of the entire PiP system. These results provide the designers of PIP systems with a deeper understanding of buckling behavior and in turn increase confidence in the robustness of such decentralized PiP systems.

Keywords: Buckling, Contact, Helical Buckling, Pipeline, Offshore, Flowline

1. Introduction

Managing wax deposition and hydrate formation in subsea flowlines containing full well stream (FWS) fluids poses a significant operational risk and capital expense for energy companies and adds significant complexity to the development of marginal hydrocarbon reservoirs. If adequate temperatures are not maintained during operation and, more crucially, shut in events, subsea FWS flowlines can become too full of wax or hydrates to flow. For some subsea flowline systems, active heating of the entire flowline is the only design alternative that can ensure that conditions can be created in the hydrocarbon fluids after long duration shut-ins.

Active heating of FWS flowlines can be provided by using electrical resistance heating of the system. Circulating hot fluid within the annulus of a pipe-in-pipe (PiP) system is another active heating method that has been used. Typical PiP configurations these heating methods are shown in Figure 1-1. When such heated PiP systems are used in deepwater applications, bulkheads and centralizers are typically used to maintain the mechanical integrity of the inner flowline during

installation and operation. The BP King project in the Gulf of Mexico is one of the more recent applications of a deepwater, heated PiP system. It uses the circulating hot fluid design, and it has centralizers. The close spacing between centralizers in a PiP system eliminates the possibility of the inner pipe to buckling in either a sinusoidal or helical mode within the outer pipe.

However, it is possible to design a PiP system where the inner flowline of the system is not constrained by centralizers. Instead, the inner flowline is free to rest along the bottom of the outer pipe. In such PiP designs there are often few, if any, centralizers in the PiP and the inner and outer pipes are fully connected only at the bulkheads at the ends. Actively heated PiP systems with no centralizers have only been installed with J-lay and S-lay installation methods. For nearly all PiP systems installed using the reeling installation method closely spaced centralizers, which eliminate helical buckling deformations, are used in the system.

The thermal expansion that occurs in such decentralized PiP systems can become very complex if moderately high temperatures are used to develop and maintain crude oil flowing temperatures. Large compressive forces can develop in the inner pipe as its expansion is resisted by both the frictional contact between the inner and outer pipes of the PiP system and the bulkheads. These compressive loads can cause the inner pipe to buckle in both a sinusoidal and, potentially, helical modes.

The study presented herein uses Abaqus to calculate the critical effective axial force (compression) needed to trigger sinusoidal and helical buckling of the inner FWS flowline within the annulus of an actively heated PiP system. The expected behavior when a pipeline is compressed within a larger diameter tubular/circular container is that it will first develop a sinusoidal buckle pattern as it lies along the bottom of the larger pipe. Further compression of the inner pipeline will ultimately cause it to snap into a helical deformation pattern, which will lift the inner pipeline off of the bottom of the outer pipeline. The axial force that triggers the sinusoidal buckling is denoted as F_{cs}, and the larger force needed for helical buckling is denoted as F_c.

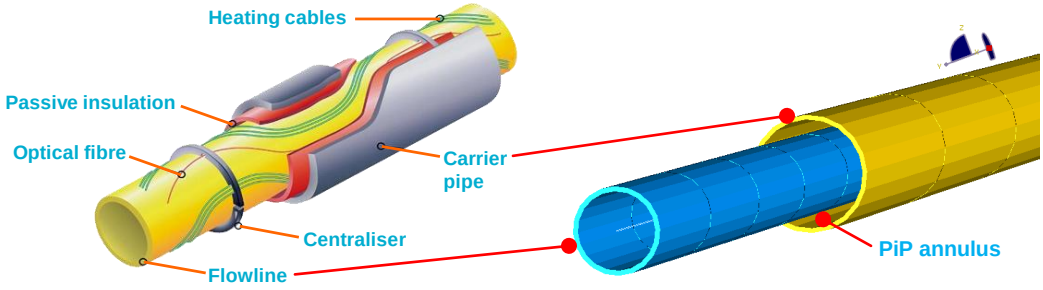

Figure 1-1 Comparison of PiP configurations for two proven active heating PiP designs

1.1 Abbreviations

CTE Coefficient of Thermal Expansion

Dof Degree of Freedom in an FE model

EAF	Effective Axial Force
EG	Ethylene Glycol Solution (Heating Fluid)
FWS	Full Well Stream
F_c	Effective Axial Force Triggering Helical Buckling of Inner Flowline
F_{cs}	Effective Axial Force Triggering Sinusoidal Buckling of Inner Flowline
FE	Finite Element (Model)
FEA	Finite Element Analysis
ID	Inside Diameter
OD	Outer Diameter
OTC	Offshore Technology Conference
PiP	Pipe-in-Pipe
SMYS	Specified Minimum Yield Strength

2. Published Analytical Models of F_{cs}

A number of researchers have studied the buckling of tubes (pipes) within circular wellbores over the past half century. Many used energy methods to derive expressions for the critical compressive loads at which the pipe will buckle within the wellbore. The two published studies that are used to guide this study are the OTC papers by Chen et al. and Huang & Pattillo. The paper by Chen et al. focused on the sub-problem of helical buckling in a horizontal wellbore, which is particularly applicable to subsea PiP systems.

Both papers note that the pipe will first buckle into a sinusoidal waveform at a critical load, denoted as F_{cs}. For a horizontal wellbore configuration, the sinusoidal waves will form along the bottom of the wellbore. As the compressive load in the tubing continues to increase, the number and amplitude of sinusoidal waves will grow until a second critical buckling load, F_c, is reached where the deformed pipe "snaps" into one or more helices along the wellbore.

Chen et al. (Chen, 1989) provide the following expressions for the two critical buckling loads:

$$F_{cs} = 2\sqrt{EIw/r}$$

$$F_c = 2\sqrt{2}\sqrt{EIw/r}$$

where,

EI is the bending stiffness of the inner pipe,

w is the inner pipeline's weight per unit length,

r is the radial gap between the inner pipe (OD) and the outer pipe (ID), assuming the two pipelines are centralized

One of the simplifying assumptions made in both of these papers is that the contact between the inner pipe and the outer circular wall is frictionless. It is noted in one of the papers (Huang, 2000) that in the "post buckling deformation of the tube in the wellbore, there is sliding of the tube on the wall of wellbore. Thus friction will play an important role." The assumption of frictionless contact is eliminated when nonlinear FE methods are used to assess the critical buckling loads of the inner flowline of a PiP sytem.

3. PIP Design Data

The geometric and material properties considered for the PiP system modeled in this study are shown in Table 3-1. The outer pipe of the system was 12.75 inch OD with a 0.5 inch wall thickness. The inner flowline pipe was 8.625 inch OD with the same wall thickness as the outer pipe. The SMYS for both pipe materials is 450 MPa. The plastic hardening curve used in the plastic material model (isotropic Mises Plasticity) for the FEA is shown in Figure 3-1. For this series of FEA, no temperature dependent plasticity data was utilized.

Table 3-1. Pipeline Geometric and Material Properties.

PROPERTY	UNITS	Flowline (inner pipe)	Carrier (outer pipe)
Nominal Pipe Size	-	8	12
Outside Diameter	mm	219.1	323.9
Nominal Wall Thickness	Mm	12.7	12.7
Steel Density	kg/m^3	7850	7850
Young's Modulus (E)	GPa	200	200
Poisson's Ratio	-	0.3	0.3
SMYS	MPa	450	450
CTE	$/C^o$	11.7e-6	11.7e-6

Table 3-2. Pipeline Operational Data.

Parameter	Unit	Flowline (inner pipe)	Outer Pipe
Design Pressure	MPa	14.5	9.25
Design Temperature	^{o}C	135	135
Hydrotest Pressure	MPa	22.00	14.75
Hydrotest Temperature	^{o}C	20	20
Max. Operating Pressure	MPa	6.0	7.5
Max. Operating Temperature	^{o}C	120	120
Weight in-air	kN/m	0.634	1.700
Submerged weight, empty	kN/m	0.634	0.055
Submerged weight, Operations	kN/m	0.515	0.795

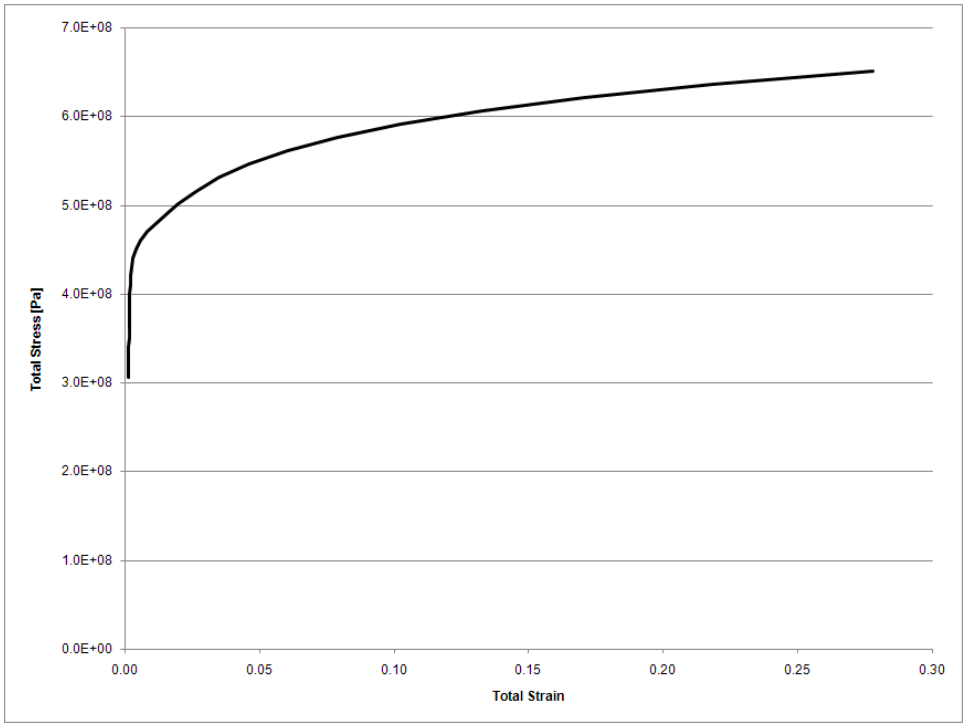

Figure 3-1. True stress – true strain data used in the Abaqus FEA.

4. Abaqus Models

4.1 Overview

The finite element simulations performed for this report used the Abaqus/Standard software program (both version 6.9-2 and 6.10-1) to obtain the solutions. The Abaqus simulations were run on an Intel workstation with 3 Gbytes of RAM and a dual 2.33 GHz CPU.

Both the inner and outer pipes of the PiP system are modeled with PIPE31 elements. The length of PiP system modeled was 1000m, and the length of each element was either 1m (for the outer pipe) or 0.5m (for the inner FWS flowline). Thus the total number of structural elements was approximately 3,000. When all of the elements needed for the contact interactions and for controlling the rotational instabilities are included, the total number of elements in the Abaqus models was between 9,000 and 9,500.

In the FE models that included the seabed and a sleeper, these structures were modeled with R3D4 elements. Contact interface models were utilized to account for the nonlinear interaction between the outer pipe and the seabed and between the outer pipe and the sleeper.

The Abaqus models use the SI system of units. Some additional details of the Abaqus models are discussed in the following sections.

4.2 Pipe-to-Pipe Contact Interaction

The complex, nonlinear contact between the inner pipe and outer pipe of the PiP system was modeled using the ITT31 element technology in Abaqus. This modeling technique allows one pipe, modeled with PIPE31 elements to slide along the ID surface of the outer pipe. Frictional models can be included in the interface behavior between the two pipe structures. Figure 4-1 shows an end view of the FE model of the 8 by 12 inch PIP model. The inner pipe is resting on the "bottom" of the outer pipe. As the two pipes slide relative to each other, frictional forces will develop both axially and circumferentially. The friction model for the pipe-to-pipe contact was isotropic. The friction coefficient was varied to study the impact of friction on the buckling response of the system.

4.3 Pipeline-Sleeper Contact

The frictional contact between the PiP system and the sleeper was assumed to be isotropic. The friction coefficient was 0.3.

4.4 Pipe-to-Seabed Contact Interaction

Pipe-soil interaction was modeled as follows. In the vertical direction, a nonlinear interaction between the depth of pipeline embedment and the vertical force exerted by seafloor was included

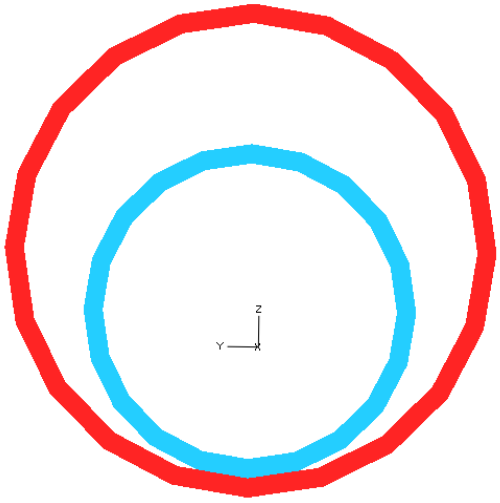

Figure 4-1 Cross section of an 8 inch by 12 inch PiP system

in the contact model between the PIPE31 elements and the R3D4 elements representing the seabed. Although pipe-soil frictional interaction models often have independent friction factors for the lateral and axial motions, in this analysis a single isotropic friction value of 0.6 was used for both the axial and lateral directions of the pipe-soil interaction.

4.5 Trigger Loads

It can be very challenging, in terms of the FEA computational cost, to get an FE simulation to "snap" into a post-buckled configuration. In the FE models used in this study, an imperfection trigger was generated in the PiP system by using a small lateral load applied to a small segment (4-6 m) of either the inner flowline (in the "completely horizontal" FE models) or the outer pipeline (in the sleeper FE model configuration). In the "completely horizontal" FE models, the magnitude of the load applied to the inner FWS pipeline was 10 N/m. In the FE models with the sleeper and seabed, the trigger load was 400 N/m and was applied to the outer pipe. A larger trigger load is needed in these FEAs because of the greater resistance of the PiP system to sliding laterally across the sleeper. In all of the models the trigger force is applied at approximately the mid span of the model.

4.6 Boundary Conditions

The boundary conditions applied to the FE models were different for the models that included the sleeper and those that did not (the "completely horizontal" models). In the "completely horizontal" Abaqus models, all of the nodes that defined the outer pipeline were held fixed in all three translational/displacement directions. The ends of the inner pipe were pinned, and one end of the inner pipe was constrained not to rotate about the longitudinal axis of the inner pipeline. The end conditions were intended to mimic those used in the analytical models for the buckling of a tubular in a horizontal wellbore.

In the sleeper models, one end of the model included a kinematic constraint to mimic the bulkhead at the end of the PiP system that ties the two pipes together. At this end of the model, the motions of the inner flowline node are required to match the displacements and rotations of the outer pipe. At the other end of the FE model, both the inner and outer pipe nodes are pinned. This end is intended to represent a point midway to the other end of the PiP system. The PiP system is allowed to contact the seabed under empty submerged weight loading conditions. From this equilibrium configuration, the sleeper is pushed up from below to seabed to raise the PiP system up off of the seabed to a specified distance. In this analysis the crown of the sleeper was placed 0.75 m above the seabed elevation. Friction between the outer pipe and the sleeper is not applied until after the sleeper has reached its final elevation. At this point the loads on the PiP system were ramped up to the operating submerged weights. In the sleeper FE models both the sleeper and seabed are not allowed to move in any direction or rotation.

The compressive loading on the inner pipe is applied by uniformly increasing the temperature of the inner pipe from its initial value. The expansion of the inner pipe is resisted by frictional forces as well as the end constraints on the inner pipe elements, which creates an effective compressive axial load (EAF) in the inner pipe.

4.7 Simulation Procedure and Convergence Controls

The buckling response of the inner pipeline of the PiP system is a highly nonlinear (and chaotic) event. The static viscous damping techniques in Abaqus/standard, which prove so helpful for many structural buckling problems where the buckling instability involves the translational Dof, are of little use for the helical buckling FEA. The "snapping" of the inner pipelineflowline into a helical configuration is dominated by the rotational Dof in the structure, and these rotational Dof are not damped with the static viscous methods. The severity and chaotic nature of the rotational instability that occurs as the inner flowline buckles in the PiP system is illustrated in Figure 4-2. In the figure, the blue curve is the rotations about the lateral axis of the FE model (which is perpendicular to the inner flowline tangent) and the orange curve is the rotation about the vertical axis of the model. The angles in the figure are given in radians.

Instead of using a static procedure for the active loading steps of the helical buckling FEA, they are solved as a nonlinear implicit dynamic transient event. However, both the physical rotary inertia created by the pipeline's mass and additional rotational damping (via discrete dashpots elements) are used in the FEA to stabilize the rotational response of the PiP system. The dashpot damping coefficients are defined as functions of scalar field variables to allow for easy tuning of the damping in the simulations. Each rotational Dof can be tuned separately. Careful evaluation of the system's rotational energies and quasi-static response prior to the initiation of buckling is used to select the dashpot coefficients.

The average simulation in this study required between 4000 and 8000 seconds to complete.

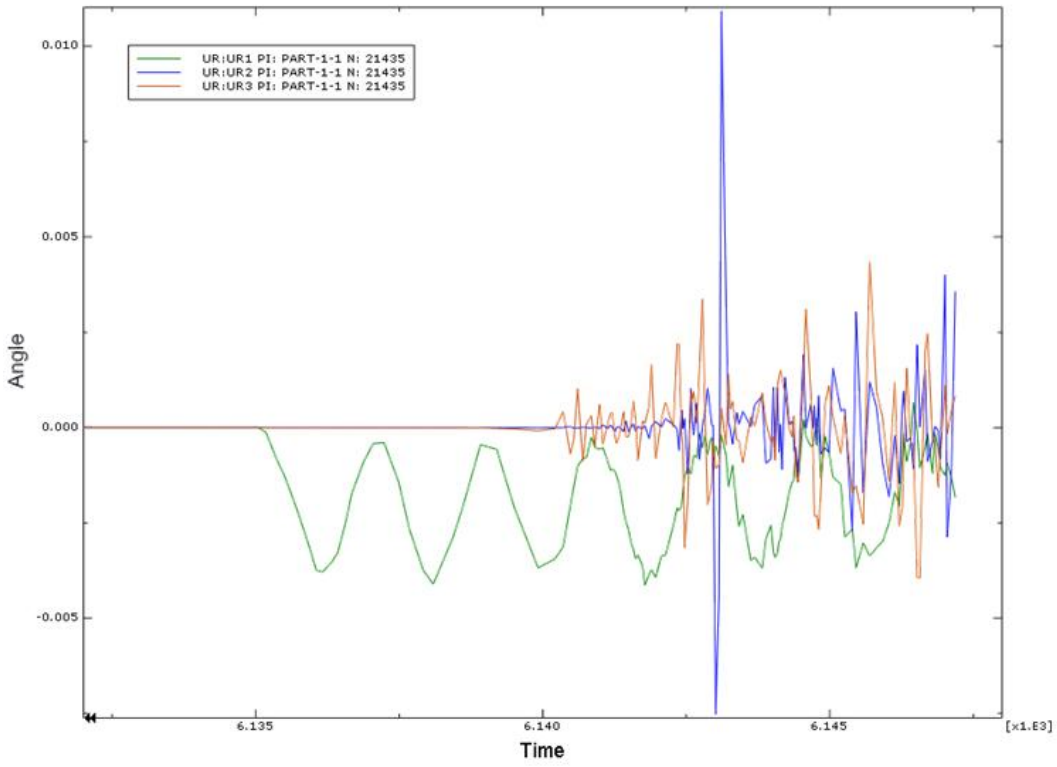

Figure 4-2. Rotational instability at a node in the inner pipeline as the loading exceeds F_c.

5. Results

5.1 Analytical Estimate of F_c

Using the expressions from Section 2 the critical load for the lower-bound onset of sinusoidal buckling (F_{cs}) of the inner FWS pipeline of the PiP is estimated to be 0.675 MN. The buckling load (F_c) required to trigger the transformation from the sinusoidal, "lateral" buckles into a helical form is estimated to be 0.954 MN. These are the buckling loads (EAF) for the inner pipe under operating conditions when there is frictionless contact between the inner and outer pipes.

5.2 Models of a Horizontal PiP

A series of FE simulations were performed using a completely horizontal configuration of the PiP system. Visualizing the post-buckling deformations for both the sinusoidal and helical buckling modes proved to be very difficult for the PiP system. The geometric imperfection, the trigger for the buckling, created in the inner pipeline is shown in Figure 5-1. The length of the inner pipe in the model (and in the figure) is 1000m and the magnitude of the imperfection shown is

approximately 3.0mm. The imperfection looks as large as it does, because of the very small angle between the axis of the pipeline and the line of sight in the image. The post-buckled deformation (sinusoidal mode at approximately F_{cs}) in this Abaqus model is shown in Figure 5-2. Friction is included in the contact behavior between the inner and outer pipelines in this Abaqus simulation. A friction coefficient of 0.1 is used in this Abaqus simulation. A much closer view of the post-buckled helical deformation that occurs in the Abaqus model is seen in Figure 5-3. The Abaqus model used to create Figure 5-3 had a pipe-pipe friction coefficient of 0.22.

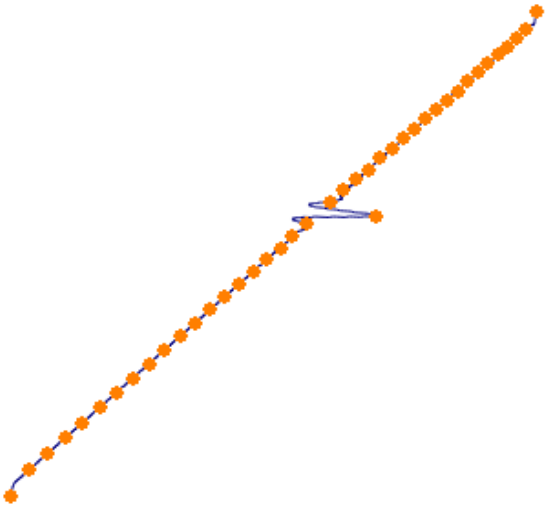

Figure 5-1. Initial imperfection of the inner pipe of the PiP system.

The impact of the friction coefficient between the inner and outer pipes on the buckling response of the inner pipe is summarized in Table 5-1. The magnitude of the F_{cs} load, which is the critical load need to trigger sinusoidal buckling of the inner pipe, is directly proportional to the pipe-pipe friction factor. The force required to initiate sinusoidal buckling in the inner pipe increased by more than 100% as the pipe-pipe friction factor increases from 0.005 (a nearly frictionless response) to a value of 0.35. Figure 5-4 shows the relationship between the pipe to pipe friction coefficient and the magnitude of F_{cs} for the inner pipe in a graphical form.

As can be seen in Table 5-1, the Abaqus model with a nearly frictionless contact interference model is able to calculate a value of F_{cs} that is within 0.75% of the value predicted by the analytical expression from Section 2. However, with even a moderately low friction factor of 0.1 the Abaqus model predicts a value of F_{cs} that is 40% higher than that estimated by the analytical expressions for frictionless contact. The results from the Abaqus models used in this study suggest that helical buckling of the inner pipe of a PiP system will become much less likely should the friction between the inner and outer pipe be below a certain magnitude, which appears to be around 0.2.

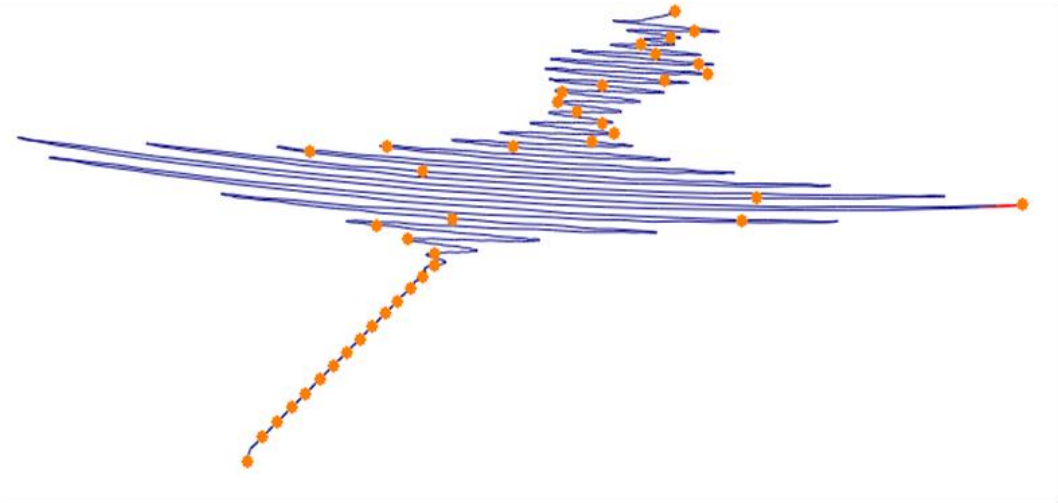

Figure 5-2. Post-buckled deformation of the inner 8 inch FWS pipeline.

The study confirms that the published analytical models for buckling of pipes inside a circular wellbore are capable of defining the theoretical lower bound value of F_{cs} for a PiP system. As shown in Figure 5-4, the analytical value of F_{cs} would need to be scaled to account for friction present in the PiP system to provide a useful estimate of the system's actual F_{cs} magnitude. It should be noted that the models used in this study are highly idealized configurations of the PiP system resting on at "flat" seabed with no displacement permitted in the outer pipe. An actual PiP system will have far more complexities to consider when evaluating the likely buckling of both the inner pipe alone and of the entire PiP system. The next section briefly describes the FE modeling performed for the PiP system in a more typical configuration for a subsea project.

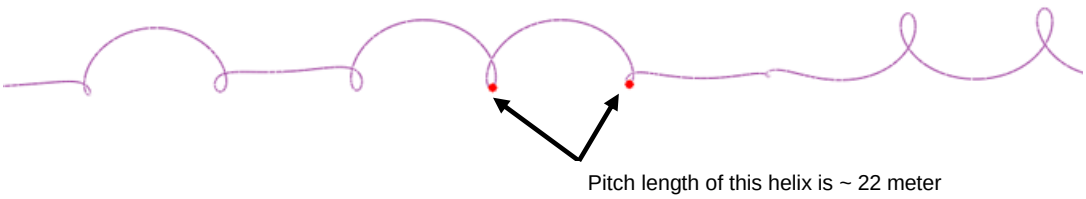

Figure 5-3. Helical buckle in the inner pipe.
(Only centerline of the pipe is shown.)

Table 5-1 Summary of F_{cs} and F_c values predicted for the PiP System

Analysis Method/Model	μ	Fcs (MN)	Fc (MN)	Comments
Analytical	0.0	0.675	0.954	Assumes horizontal, frictionless wellbore.
FEA / Horizontal Model	0.35	1.46	1.46	Transition from sinusoidal to helical buckling occurs immediately
FEA / Horizontal Model	0.22	1.21	1.22	
FEA / Horizontal Model	0.15	1.06	1.06	Loading never reached F_c level
FEA / Horizontal Model	0.1	0.944	NA	Loading never reached F_c level
FEA / Horizontal Model	0.08	0.894	NA	Loading never reached F_c level.
FEA / Horizontal Model	0.01	0.72	NA	Loading never reached F_c level
FEA / Horizontal Model w. nearly Frictionless Contact	~0.0	0.680	NA	Friction Coefficient is 0.005.
FEA/ Single 0.75 m Sleeper with flat Seabed	0.35	0.90	NA	Inner pipeline does not reach F_c loads. Pipe-Sleeper Friction Coefficient: 0.3

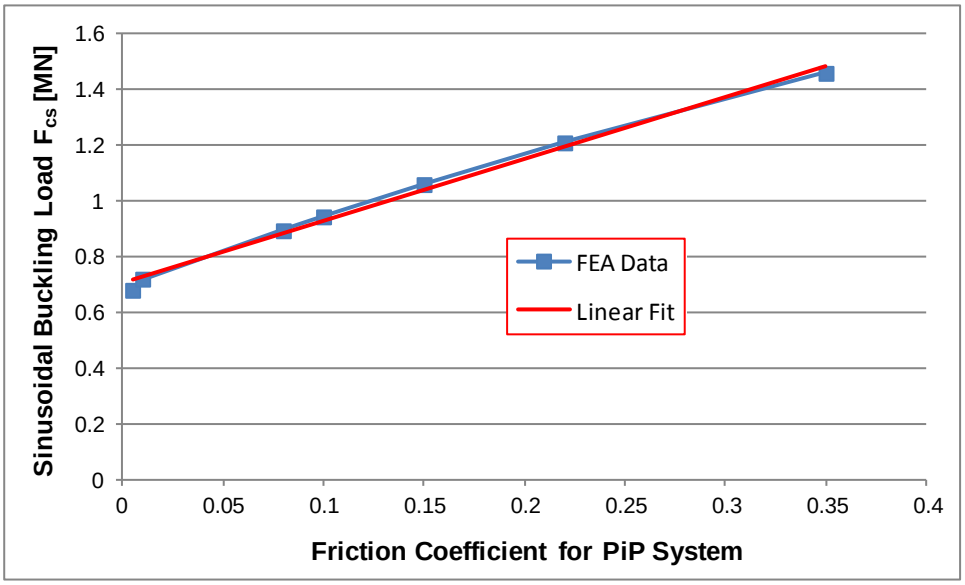

Figure 5-4. Impact of pipe-pipe friction on F_{cs}

5.3 Models of the PiP System Crossing a Single Sleeper

Sleepers that lift a subsea pipeline up off of the seabed are used to provide an engineered trigger for lateral buckles as a mitigation method for thermal expansion effects experienced during operational loading. In the Abaqus simulation the top of the sleeper was 0.75 m above the seabed surface. In this simulation the seabed was still considered flat. A friction coefficient of 0.35 was used between the inner pipe and the outer pipe in the simulation. The friction coefficient between the outer pipe and the sleeper was 0.3. An initial lateral deflection of approximately 0.01m was created with a triggering force, as can be seen by the dark blue curve in Figure 5-5. This imperfection is created to help trigger the buckling response in the FEA. The growth of the buckling response of the inner pipe as the temperature of the inner pipe is increased from an initial value of 20^{o} C to a final value of 120^{o} C is also shown in the figure. The radial clearance shown in Figure 5-5 provides an indication of when the inner pipe has "forced" a global deflection of the PiP. At lower thermal loads, the buckles of the inner pipe have just pushed up along the ID surface of the outer pipe. However at the final load shown in this figure (curve "0-5084"), the inner pipe has pushed far beyond the radial clearance, indicating that it has pushed the outer pipe along as it buckles. This is clearly seen in the deformed shape plots in Figure 5-6.

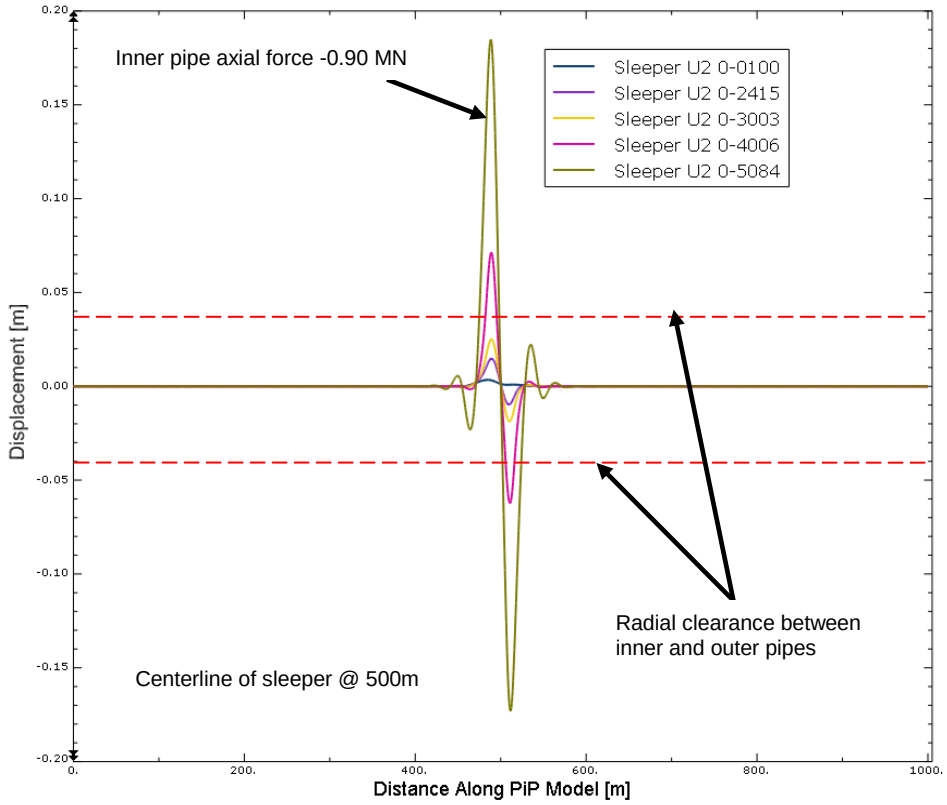

Figure 5-5. Lateral Displacements of the inner pipe of the PiP system as the global buckle forms under thermal loading.

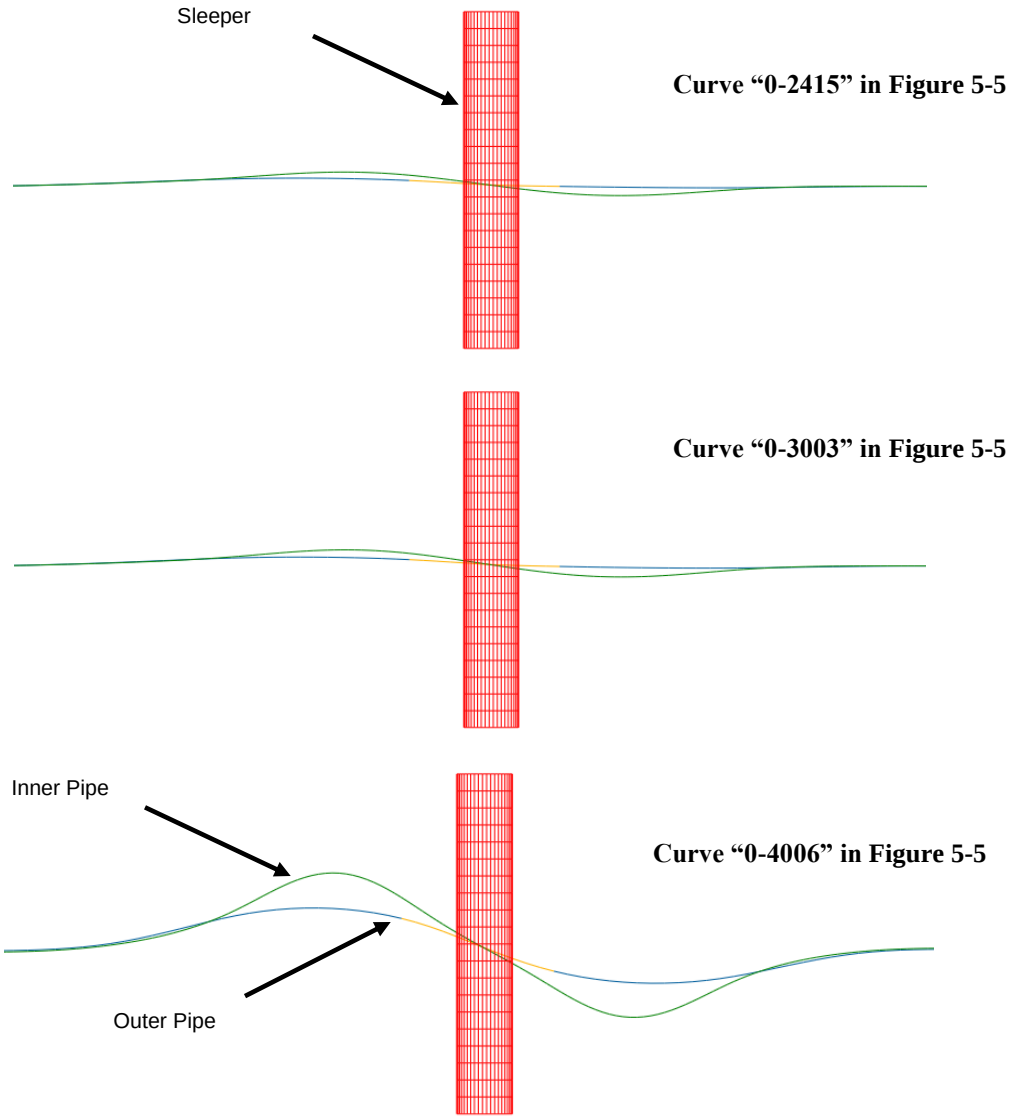

Figure 5-6. Evolution of the deformations of the PiP system at the sleeper location. Deformations use 100x magnification.

6. Summary & Conclusions

Nonlinear FEA models of decentralized PiP systems were used to investigate the buckling response of the inner pipe within the outer pipe. The FEA methodology can simulate the complex deformation associated with helical buckling of the inner pipe and was able to predict values for F_{cs} and F_c very similar to those calculated using published analytical expressions for buckling of tubular members in horizontal wellbores. However, significant simplifications as compared to actual subsea pipeline configurations and operating conditions, namely frictionless contact between the inner and outer pipes and a flat seabed, had to be used because of the limits of the published analytical models. The friction between the inner and outer pipes has a very significant effect on the ability of the inner pipe to buckle (in either sinusoidal or helical modes) within the outer pipe. The magnitude of F_{cs} increases as the friction coefficient between the two pipes of the PiP system is increased.

The pipe-to-pipe frictional behavior in a PiP system is just one of several input parameters that have a profound impact on the global lateral buckling response of such PiP systems. Other equally important parameters are the initial EAF profiles in the system, the pipe-soil interaction modeling, the vertical geometric imperfections (from seabed features) and the horizontal geometric imperfections. The intention of this study was to isolate, as much as possible, the buckling response of a PiP system from these other variables so that only the impact of pipe-pipe friction could be assessed. Such isolation is impossible in as-installed evaluations and even difficult in small scale physical models.

Sinusoidal buckling of the inner pipeline can create enough lateral loads on the outer pipe of the PiP system to cause a global lateral buckle when the PiP pipeline is on top of a sleeper. Such large global deformations of the PiP system reduce the probability that helical buckles will form, by reducing the effective axial force in the inner pipe of the PiP system after lateral deflection. These results provide the engineers designing the PiP systems with a deeper understanding of buckling behavior and in turn increase confidence in the robustness of the design of such PiP systems.

Most of the PiP systems have used centralizers to hold the inner pipe in a, more or less, coaxial alignment with the outer pipe. The presence of such centralizers eliminates the possibility of the inner pipe to buckling within the outer pipe in either a sinusoidal of helical mode.

7. References

1. Y.C. Chen, Y.H. Lin and J.B. Cheatham, “An Analysis of Tubing and Casing Buckling in Horizontal Wells (OTC 6037),” OTC 6037, May 1989.
2. N.C. Huang, P.D. Pattillo “Helical Buckling of a tube in an Inclined Wellbore,” International Journal of Non-Linear Mechanics, 2000.